

The Role of Vesicular Glutamate Transporter Type 3 in Social Behavior, with a Focus on the Median Raphe Region

Csilla Lea Fazekas,^{1,2,3} Bibiána Török,² Pedro Correia,^{1,2,3} Tiago Chaves,^{1,2,3} Manon Bellardie,² Eszter Sipos,² Hanga Réka Horváth,² Balázs Gaszner,⁴ Fanni Dóra,^{5,6}  Árpád Dobolyi,^{6,7} and Dóra Zelena^{1,2}

¹Institute of Physiology, Medical School, Centre for Neuroscience, Szentágotthai Research Centre, University of Pécs, Pécs 7624, Hungary, ²Institute of Experimental Medicine, Eötvös Loránd Research Network, Budapest 1084, Hungary, ³János Szentágotthai Doctoral School of Neurosciences, Semmelweis University, Budapest 1085, Hungary, ⁴Department of Anatomy, Medical School, Centre for Neuroscience, Szentágotthai Research Centre, University of Pécs, Pécs 7624, Hungary, ⁵Human Brain Bank and Microdissection Laboratory, Semmelweis University, Budapest 1085, Hungary, ⁶Laboratory of Neuromorphology, Department of Anatomy, Histology and Embryology, Semmelweis University, Budapest 1085, Hungary, and ⁷Laboratory of Molecular and Systems Neurobiology, Department of Physiology and Neurobiology, Eötvös Loránd University, Budapest 1117, Hungary

Received Aug. 30, 2023; revised March 27, 2024; accepted April 8, 2024.

The authors declare no competing financial interests. The agencies had no further role in study design and in the collection, analysis, or interpretation of the data.

Author contributions: C.L.F., B.T., A.D., and D.Z. designed research; C.L.F., B.T., P.C., T.C., M.B., E.S., H.R.H., B.G., F.D., and D.Z. performed research; C.L.F., B.T., P.C., T.C., M.B., E.S., H.R.H., B.G., F.D., A.D., and D.Z. analyzed data; C.L.F., B.T., A.D., and D.Z. wrote the paper.

We thank the Behavioral Studies Unit at the IEM for providing the appropriate environment for keeping laboratory animals and conducting experiments. We thank the Nikon Centre of Excellence at IEM, Nikon Austria and Auro-Science Consulting for kindly providing microscopy support. This work was supported by the Thematic Excellence Program 2021 Health Sub-program of the Ministry for Innovation and Technology in Hungary, within the framework of the TKP2021-EGA-16 project of Pécs of University and by the Hungarian Brain Research Program 3.0 (NAP 3.0) 2022–2025, the National Research Development and Innovation Office of Hungary (grant numbers K141934, K138763, K120311, K134221), the New National Excellence Program of the Ministry of Human Capacities (ÚNKP-18-1).

Continued on next page.

Abstract

Social behavior is important for our well-being, and its dysfunctions impact several pathological conditions. Although the involvement of glutamate is undeniable, the relevance of vesicular glutamate transporter type 3 (VGLUT3), a specific vesicular transporter, in the control of social behavior is not sufficiently explored. Since midbrain median raphe region (MRR) is implicated in social behavior and the nucleus contains high amount of VGLUT3+ neurons, we compared the behavior of male VGLUT3 knock-out (KO) and VGLUT3-Cre mice, the latter after chemogenetic MRR-VGLUT3 manipulation. Appropriate control groups were included. Behavioral test battery was used for social behavior (sociability, social discrimination, social interaction, resident intruder test) and possible confounding factors (open field, elevated plus maze, Y-maze tests). Neuronal activation was studied by c-Fos immunohistochemistry. Human relevance was confirmed by VGLUT3 gene expression in relevant human brainstem areas. VGLUT3 KO mice exhibited increased anxiety, social interest, but also aggressive behavior in anxiogenic environment and impaired social memory. For KO animals, social interaction induced lower cell activation in the anterior cingulate, infralimbic cortex, and medial septum. In turn, excitation of MRR-VGLUT3+ neurons was anxiolytic. Inhibition increased social interest 24 h later but decreased mobility and social behavior in aggressive context. Chemogenetic activation increased the number of c-Fos+ neurons only in the MRR. We confirmed the increased anxiety-like behavior and impaired memory of VGLUT3 KO strain and revealed increased, but inadequate, social behavior. MRR-VGLUT3 neurons regulated mobility and social and anxiety-like behavior in a context-dependent manner. The presence of VGLUT3 mRNA on corresponding human brain areas suggests clinical relevance.

Key words: chemogenetic; median raphe; social behavior; VGLUT3; VGLUT3-Cre mice; VGLUT3 knock-out mice

Significance Statement

The control of social behavior is complex, and the role of numerous subcortical areas in it is still poorly understood. In our experiments, we investigated a subpopulation of glutamatergic neurons that express the vesicular glutamate transporter type 3 (VGLUT3), especially those found in the median raphe region

(MRR) in the control of social behavior, locomotion, anxiety, and memory. In mice completely lacking VGLUT3, the highly anxious behavior, alterations in locomotion, and impaired memory were confirmed, and increased social interest and inadequate aggressive behavior were also revealed. MRR-VGLUT3 neurons proved to be at least partially responsible for the locomotor and anxiety-like behavior, as well as social interest. Lastly, translational relevance was proved by detection of the VGLUT3 gene expression in the human brainstem.

Introduction

Vesicular glutamate transporter type 3 (VGLUT3) is the latest transporter discovered from the solute carrier (SLC) 17 protein family (Fremeau et al., 2002), and thus, its role in behavior is still largely unknown. Homozygous VGLUT3 knock-out (KO) mice are viable (Horvath et al., 2018) and their behavioral characterization is ongoing (Seal et al., 2008; Amilhon et al., 2010; Divito et al., 2015; Balazsfi et al., 2016, 2018a; Fazekas et al., 2019). However, detailed investigation of its contribution to social behavior is still missing, despite the importance of these interactions in everyday life as well as its disturbances in psychopathologies.

Numerous brain regions contain VGLUT3-positive neurons, such as the hippocampus, cortex, and median raphe region (MRR) in the midbrain. The MRR is known as one of the serotonergic nuclei, which provides serotonergic innervation to the forebrain (Dahlstrom and Fuxe, 1964; Vertes et al., 1999). However, only 5.742% of the MRR neurons have been shown to express serotonin (5-HT; Sos et al., 2017). The rest of the cells express numerous other neurotransmitters and neuromodulators, such as GABA (Calizo et al., 2011; Sos et al., 2017), dopamine (Jahanshahi et al., 2013), and glutamate, characterized by VGLUT2 (Szonyi et al., 2019) or VGLUT3 (Fremeau et al., 2002; Herzog et al., 2004; Amilhon et al., 2010; Sos et al., 2017). According to our current knowledge, ~10.651% of the MRR cells contain VGLUT3 as a neuronal marker, while ~3.603% of the MRR cells show serotonin and VGLUT3 coexpression as well (Sos et al., 2017). These VGLUT3-positive cells target key areas such as the medial prefrontal cortex (mPFC), hippocampus, thalamus, hypothalamus, and dorsal raphe (Jackson et al., 2009; Szonyi et al., 2016). Numerous studies have investigated the role of MRR in behavior (Wang et al., 2015; Bland et al., 2016; Balazsfi et al., 2017; Turcotte-Cardin et al., 2019), but they were solely concentrating on its serotonergic content. However, it was demonstrated that at least in certain areas (e.g., mPFC, hippocampus, medial septum), functional glutamate receptors are expressed in the postsynaptic sites of these MRR-VGLUT3-positive projections (Szonyi et al., 2016). The optogenetic stimulation of the whole MRR decreased aggressive behavior in a phasic manner in mice, which was accompanied by increased serotonergic, GABAergic, and glutamatergic neurotransmitter levels in the mPFC (Balazsfi et al., 2018b). While it is established that MRR regulates social behavior, the specific role of its VGLUT3+ neurons is still unknown.

Our aim was to characterize the role of VGLUT3 in social behavior. With the usage of VGLUT3 knock-out (KO) mice, the global role of this transporter could be revealed; however, life-long, constitutive lack of a gene product could result in compensatory mechanisms, ultimately masking behavioral effects. The chemogenetic manipulation of MRR-VGLUT3 neurons would shed new light on the role of this specific subpopulation giving the opportunity for both stimulatory and inhibitory short-term interventions. The comparison of the two models would provide deeper insight on the role of VGLUT3.

Materials and Methods

Animals

All mice (C57BL/6J background) were obtained from the local colonies of the Institute of Experimental Medicine, Budapest, Hungary. VGLUT3 wild-type (WT) and KO mice were bred in heterozygous mating pairs. Their genotype was determined by PCR from a small tail sample collected from 2- to 3-day-old animals. VGLUT3-Cre mice originated from homozygous mating. During the test battery adult male mice (14–15-week-old) were housed in Makrolon cages (40 cm × 25 cm × 26 cm) under a “reversed” 12 h light/dark cycle (lights on at 7 P.M., 21 ± 1°C, 50–60% humidity), with food (standard mice chow, Charles River) and tap water available *ad libitum*. Thirty minutes before the start of the first experiment, the animals were separated to increase social interest during subsequent

Correspondence should be addressed to Dóra Zelena at zelena.dora@pte.hu.

Copyright © 2024 Fazekas et al. This is an open-access article distributed under the terms of the Creative Commons Attribution 4.0 International license, which permits unrestricted use, distribution and reproduction in any medium provided that the original work is properly attributed.

testing. The experiments were conducted between 9 and 13 h, during the subjective dark period of the mice. The KO-WT and VGluT3-Cre animals were tested in different series with minor differences in the protocol (Fig. 1A):

1. Series 1: WT ($N = 10$) and VGluT3 KO ($N = 11$) animals were compared.
2. Series 2: VGluT3-Cre animals went under stereotaxic surgery. Three subgroups were formed based on the injected viral vectors containing “designer receptors exclusively activated by designer drug” (DREADD) sequences: control ($N = 8$), excitatory ($N = 13$), and inhibitory ($N = 15$).

c-Fos activation was studied in a different batch of animals from those used in the behavioral studies. Wild-type ($N = 5$) and VGluT3 KO ($N = 8$) mice were perfused 90 min after a social interaction test (SIT). In the case of VGluT3-Cre mice ($N_{\text{control}} = 6$; $N_{\text{excitatory}} = 3$), separate animals were injected intraperitoneal (i.p.) with clozapine-*N*-oxide (CNO, ligand of DREADD; CAS No.: 34233-69-7, Tocris Bioscience, 1 mg/kg/10 ml saline) and perfused 30 (time for CNO to take effect) + 90 min (c-Fos expression peak) after injection.

All tests were approved by the local committee of animal health and care (PEI/001/33-4/2013, PE/EA/254-7/2019) and performed according to the European Communities Council Directive recommendations for the care and use of laboratory animals (2010/63/EU).

Surgery

Anesthetized [0.1 ml/10 g mixture of 0.5 ml ketamine (Produlab Pharma), 0.1 ml xylazine (Produlab Pharma), and 2.4 ml saline (KabiPac)] VGluT3-Cre mice were stereotaxically (David Kopf Instruments) injected with an adeno-associated virus vector (AAV8) containing DREADD and/or red fluorescent protein (RFP) sequences between two loxP loci (20 nl; Addgene) into the MRR (AP: -4.1 mm; L: 0 mm; DV: 4.6 mm from bregma; Balazsfi et al., 2017, 2018b; Fazekas et al., 2021; Chaves et al., 2022). Three groups were formed: control (only RFP; #50459); excitatory (G_q stimulation; #44361), and inhibitory (G_i inhibition; #44362). Animals had 28 d to recover, of which they adapted to the reverse cycle for 14 d.

Experimental design

Thirty minutes before the experiments (except for social discrimination test; SDT), VGluT3-Cre animals were injected intraperitoneally with CNO (Chaves et al., 2022). There were 48–72 h intervals between behavior tests (except for SDT) to ensure the clearance of previously injected CNO (Fig. 1A). For comparability the timing was the same in both series.

The experimental room was dark, only lit by infrared light [except for SIT and elevated plus maze (EPM)]. The experiments were recorded and analyzed later by computer-based event recorders (H77; Solomon Coder (<https://solomoncoder.com>); Noldus EthoVision). The test apparatuses were cleaned with 20% ethanol between animals except for SIT and RIT (with bedding).

In the end, the animals were anaesthetized by ketamine–xylazine and fixed by transcardial perfusion with phosphate-buffered saline (PBS; Molar Chemicals) and 4% paraformaldehyde (PFA; Molar Chemicals). After 24 h postfixation in PFA, the solution was changed to azide-PBS (Na-azide from Sigma-Aldrich). Before cutting, the brains were immersed in 20% glucose (Reanal) azide-PBS for at least 24 h. Thirty-micrometer slices were cut with sledge microtome and stored in cryoprotectant (all components from Molar Chemicals) at -20°C . Immunohistochemistry was done for RFP and VGluT3 in order to validate the virus expression (Fig. 1B) and cell specificity (Fig. 1C). Staining for c-Fos was conducted to explore neuronal activity.

Open field. Open field (OF) measures the locomotor activity and anxiety-like behavior of mice. Animals were put into an empty white plastic box (40 cm \times 36 cm \times 15 cm; Fig. 2A). Distance traveled, frequency, and time spent in periphery and centrum (75% of the arena) were analyzed by the Noldus EthoVision XT 13.

Sociability. Right after OF, two identical wired cages (with identical weights on them) were placed into the empty plastic boxes (object habituation phase; Fig. 2A). Based on their location, they were either labeled as “left” or “right.” After 5 min, an unknown, smaller, juvenile male conspecific was placed under one of the cages for 5 min (sociability phase).

Social preference index (SI) was calculated as follows:

$$\text{SI} = \frac{t_{\text{mouse}}}{t_{\text{mouse}} + t_{\text{cage}}} \times 100,$$

where t_{mouse} is the time spent sniffing the stimulus mouse; t_{cage} is the time spent sniffing the empty cage.

Any other type of behavior was labeled as “other.”

Social discrimination. Twenty-four hours after sociability test, SDT was conducted. The experimental setting was identical to that of sociability (Fig. 2A). Under each wired cage, a conspecific was placed for 5 min. One was used during

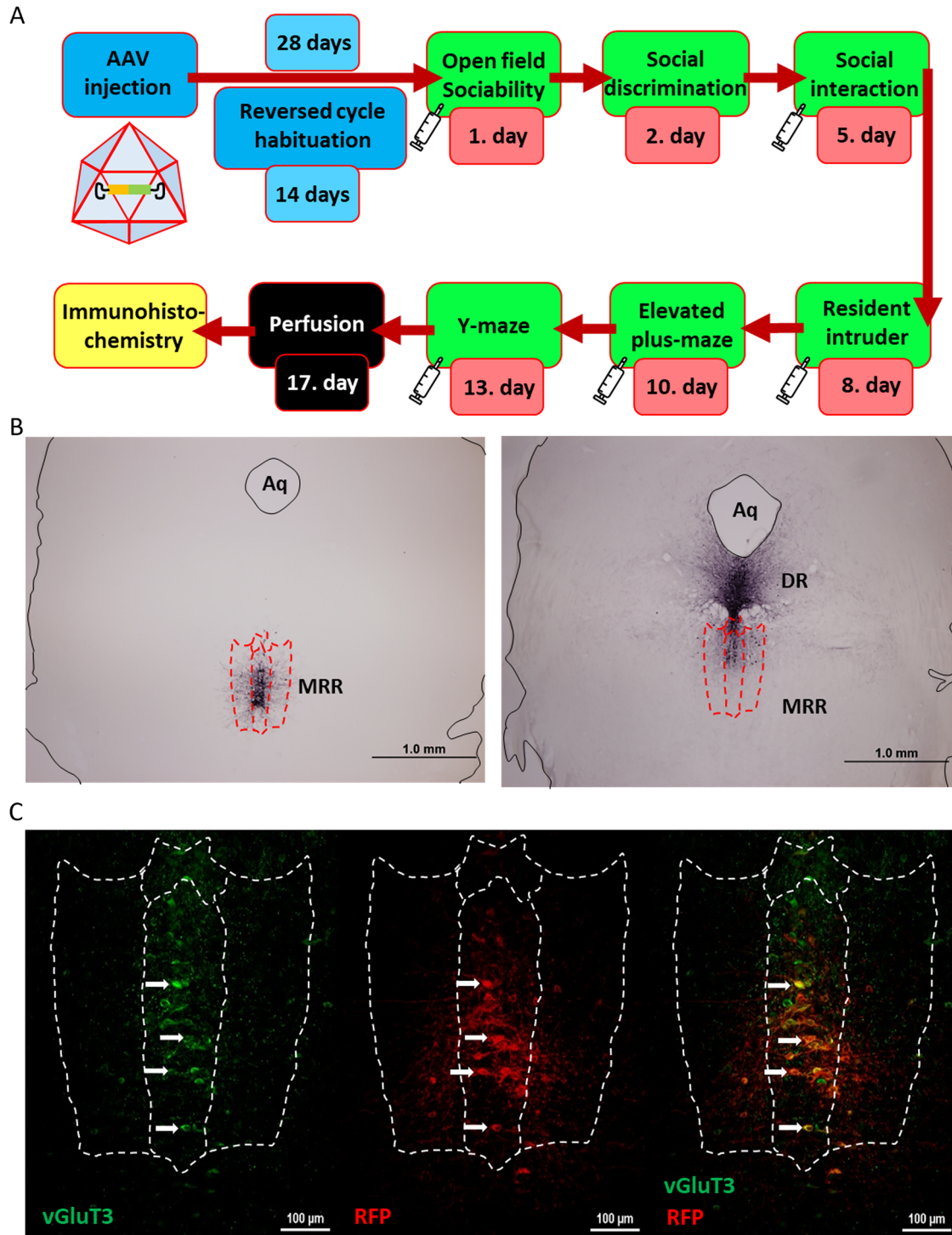


Figure 1. Timeline of the experimental protocols and immunohistochemical validation. **A**, Schematic timeline of the behavioral test battery. In case of VGlut3-Cre mice, experiments started 4 weeks after the stereotaxic surgery—which included 2 weeks of habituation to “reversed” day/night cycle—in order to ensure viral expression of DREADDs. Syringes indicate the occasions when VGlut3-Cre mice were injected intraperitoneally with CNO (1 mg/ml/kg) 30 min before the start of the experiment. Two to 3 d of break were kept between the experiments in order to eliminate the carry-over effect of CNO. WT and VGlut3 KO mice went under the same procedure, except for the surgery and CNO administration. **B**, Example of proper (left) and improper (right) viral expression in VGlut3-Cre mice. After the experiments, brains were collected from the animals, and Ni-DAB staining was done on midbrain slices against the RFP encoded in the AAV. Only the data of those animals that had proper viral expression in the MRR were included in the statistical analysis. On the right, there is an example of unacceptable staining in the DR. **C**, Representative figure of viral expression specificity in the MRR. Double fluorescent immunohistochemistry was done of midbrain slices against VGlut3 (Alexa-488, green) and RFP (Alexa-594, red) in control virus injected VGlut3-Cre mice. White arrows indicate example neurons where both markers were found. Scale bar, 100 μ m. AAV, adeno-associated virus vector; Aq, Aqueduct cerebri; CNO, clozapine-*N*-oxide; DR, dorsal raphe; DREADD, designer receptor exclusively activated by designer drugs; KO, knock-out; MRR, median raphe region; Ni-DAB, nickel-3,3'-diaminobenzidine; RFP, red fluorescent protein; VGlut3, vesicular glutamate transporter 3; WT, wild-type.

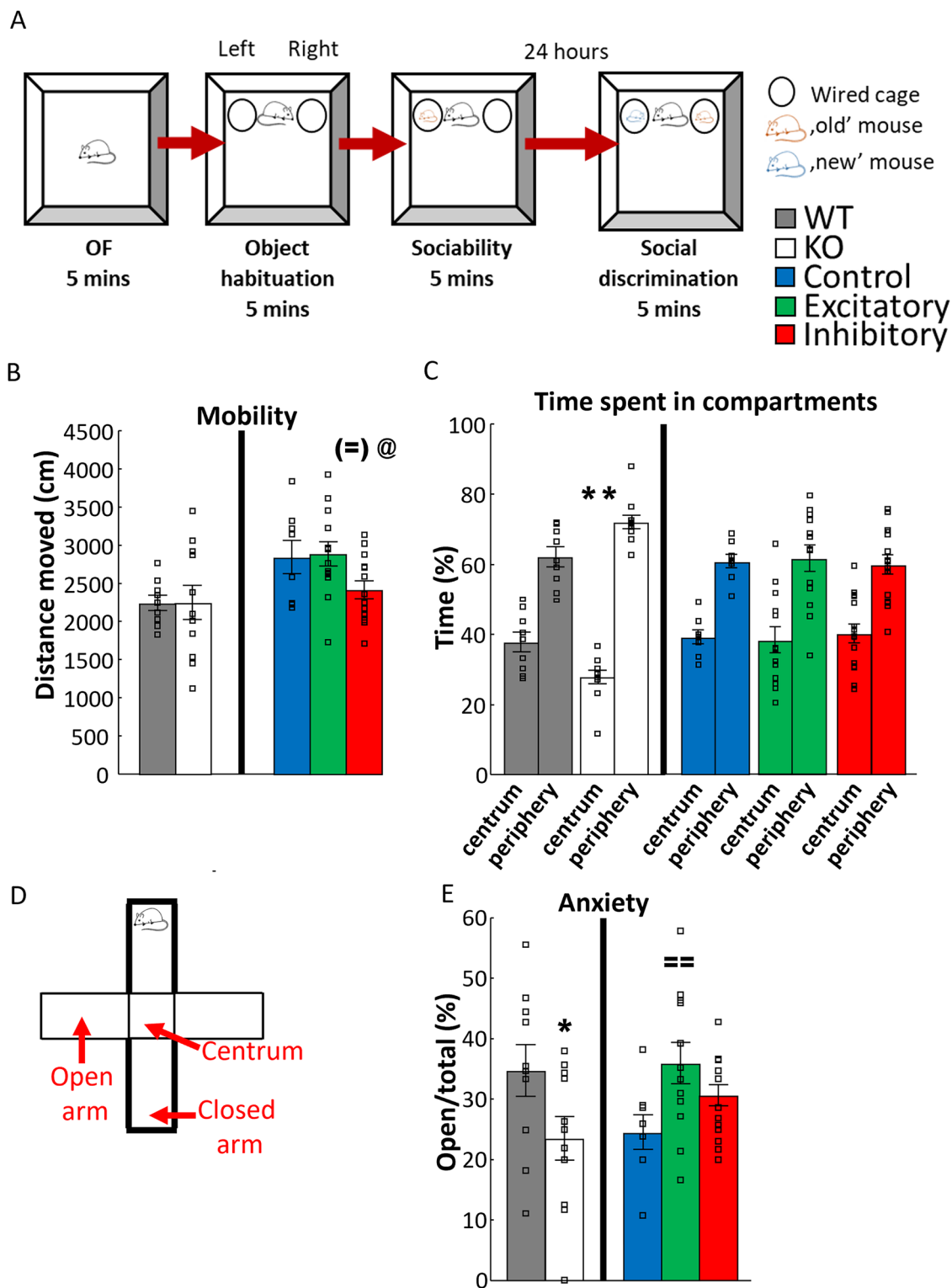


Figure 2. Results of experiments on mobility and anxiety-like behavior. **A**, Schematic figure of sociability test, which started with a 5 min of OF test for mobility and anxiety-like behavior. Right after that, 5 min of object habituation followed when two identical wired cages were put into the arena. Right after that, one unfamiliar, juvenile conspecific was put under one of the wired cages for sociability phase. One day later, a 5 min SDT was conducted, during which the already familiar and a new unfamiliar conspecific were placed under the wired cages with interchanged positions compared with the previous day. **B**, Distance moved during OF. In dark, there was no difference between WT and VGLuT3 KO mice (*t* test, $N_{WT} = 9$; $N_{KO} = 11$). On the other hand, inhibition of VGLuT3+ neurons in the MRR resulted in decreased mobility (one-way ANOVA; $N_{control} = 8$; $N_{excitatory} = 13$; $N_{inhibitory} = 14$). **C**, Percentage of time in different zones during OF. Increased anxiety-like behavior (repeated-measures ANOVA) in VGLuT3 KO mice is reflected by decreased time spent in the centrum (75% of the arena floor). **D**, Schematic representation of EPM apparatus. EPM consists of two closed arms and two open arms connected by a centrum area, elevated 67 cm above the ground. **E**, Open/total (%) is a locomotion independent parameter that reflects anxiety-like behavior on

sociability (“old”), while the other one was unknown (“new”). Here CNO was not injected; thus, the effect on memory consolidation and not on recall was tested.

Social discrimination index (SD) was calculated as follows:

$$SD = \frac{t_{\text{“old”}} - t_{\text{“new”}}}{t_{\text{“old”}} + t_{\text{“new”}}} \times 100,$$

where $t_{\text{“old”}}$ is the time spent sniffing the familiar stimulus mouse; $t_{\text{“new”}}$ is the time spent sniffing the unfamiliar stimulus mouse.

Social interaction. The test was conducted in a transparent Plexiglass chamber (35 cm × 20 cm × 25 cm, Geo Maxi mini aquarium) with bedding (Fig. 3C). On previous day mice were put into the respective chamber for 2 × 15 min, 4 h apart, for habituation. During the experiment, two animals from the same group (e.g., KO vs KO), roughly weighting the same, were put into the chamber. The mice could freely behave for 10 min under normal lighting.

Social (e.g., sniffing), aggressive (e.g., biting, aggressive dominance), and defensive behaviors were analyzed for both test animals. Any other type of behavior was labeled as “other.”

Resident intruder. An unfamiliar, physically smaller, but adult conspecific was put into the home cage of the test animals. For 10 min, the animals could freely behave (Fig. 3D). Only the behavior of the test animal was analyzed (with similar parameters as in case of SIT).

EPM. The animals were placed onto the middle, central zone of the EPM apparatus (height, 25 cm; width, 7 cm; length, 30 cm; 67 cm above the floor) with two open and two closed arms aimed to measure anxiety (Fig. 2D). The mice could behave freely for 5 min in bright light (120 lux).

Open arm entries reflecting mobility independent anxiety were calculated:

$$\frac{\text{Open}}{\text{Total}} (\%) = \frac{\text{Number of open arm entries}}{\text{Sum of open + closed arm entries}}.$$

The frequency of risk assessment (RA) behavior (head dipping, stretched attend posture, and rearing) and grooming were also evaluated.

Y-maze. This test detects the short-term learning and memory of rodents, reflected by continuous spontaneous alternation (Hughes, 2004). The apparatus consists of three arms (A, B, and C; 25 cm × 5 cm × 21 cm) at 120°, connected by a central zone (Fig. 4C). No extra external spatial cues were used during the experiment. The consecutive arm entries reflect intact short-term memory. Mice were placed at the end of arm A and were allowed to explore the maze freely for 5 min.

Spontaneous alternation was calculated as follows:

$$\text{Spontaneous alternation} = \frac{\text{“correct” alternation}}{\text{sum of all arm entries} - 2} \times 100,$$

where “correct” alternation is the entry into all three arms on consecutive choices (i.e., ABC, but not CAC; Fazekas et al., 2019; Chaves et al., 2022).

Immunohistochemistry and microscopy

In VGlut3-Cre mice, virus infection and expression had to be validated. Nickel-3,3'-diaminobenzidine (Ni-DAB, Sigma-Aldrich) staining was conducted on midbrain slices containing MRR (Biro et al., 2017; Chaves et al., 2022). The slices were incubated in anti-RFP primer solution (1:4,000, rabbit, #600-401-379, Rockland) for two nights on 4°C. The secondary solution consisted of biotinylated (biotin-SP) anti-rabbit antibody (1:1,000 donkey, #711-065-152, Jackson). The signal was strengthened by avidin-biotin complex (1:1,000, ABC; Vector Laboratories) and then developed in the presence of DAB (10 mg/ml) and 1% NiNH₄SO₄ (Sigma-Aldrich) and H₂O₂ (Sigma-Aldrich). The mounting was done in gelatine (G9391, Sigma-Aldrich), and then the slides were dehydrated in xylol and covered with DPX (Sigma-Aldrich).

←
EPM. Increased anxiety-like behavior is reflected by decreased open/total (%) in VGlut3 KO mice (t test; $N_{\text{WT}} = 10$; $N_{\text{KO}} = 11$). On the other hand, the excitation of MRR-VGlut3+ neurons elicited anxiolytic effect (one-way ANOVA; $N_{\text{control}} = 8$; $N_{\text{excitatory}} = 15$; $N_{\text{inhibitory}} = 15$). Data are expressed as average ± SEM. Empty squares represent individual values. For more details see Extended Data Tables to Figure 2. EPM, elevated plus maze test; KO, knock-out; MRR, median raphe region; OF, open field test; VGlut3, vesicular glutamate transporter type 3; WT, wild-type. ** $p < 0.01$ versus WT; ⁽⁻⁾ $p = 0.08$, ⁽⁼⁾ $p < 0.01$ versus control; ^(*) $p < 0.05$ versus excitatory.

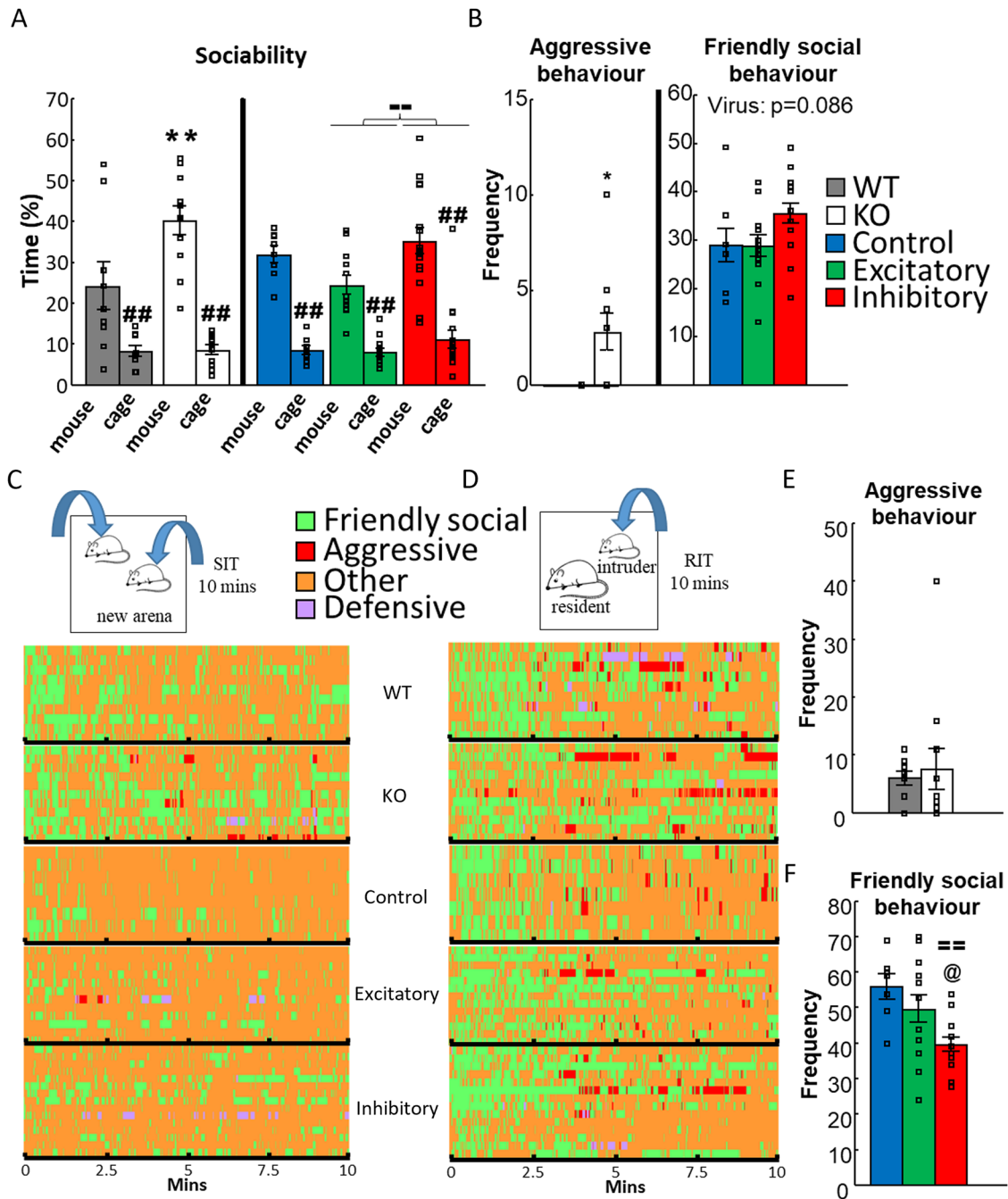


Figure 3. Results of experiments on social behavior. **A**, Percentage of time spent with empty cages and the cage containing an unfamiliar, juvenile conspecific. Both WT and VGLuT3 KO mice preferred the social stimuli compared with the inanimate object, but KO animals spent more time with the conspecific (repeated-measures ANOVA; $N_{WT} = 10$; $N_{KO} = 11$). Similarly, all animals in the VGLuT3-Cre groups preferred the social stimuli, but the excitatory group had decreased interest compared with the inhibitory group (repeated-measures ANOVA; $N_{control} = 8$; $N_{excitatory} = 11$; $N_{inhibitory} = 15$). **B**, Main differences between groups in SIT. VGLuT3 KO mice exhibited more aggressive behavior compared with the WT animals (t test; $N_{WT} = 10$; $N_{KO} = 11$). On the other hand, friendly social behavior was only marginally changed in the VGLuT3-Cre mice (one-way ANOVA; $N_{control} = 8$; $N_{excitatory} = 13$; $N_{inhibitory} = 15$). **C**, Schematic representation of SIT protocol: for 10 min two experimental animals from the same treatment group (e.g., KO vs KO, excitatory vs excitatory) was placed into a neutral, anxiogenic environment to freely interact. Under the figure Gantt diagrams visually represent the behavior of all experimental animals during SIT. Different behaviors are represented by different colors. **D**, Schematic representation of RIT protocol: for 10 min an unfamiliar, physically smaller, but adult conspecific was placed into the home cage of the experimental mouse to freely interact. Under the figure Gantt diagrams visually represent the behavior of all experimental animals during RIT. Different behaviors are represented by different colors. **E**, Frequency of aggressive behavior did not differ between WT and VGLuT3 KO mice during RIT (t test; $N_{WT} = 10$; $N_{KO} = 11$). **F**, Frequency of friendly social behavior was decreased in the inhibitory group of VGLuT3-Cre mice in RIT (one-way ANOVA; $N_{control} = 8$; $N_{excitatory} = 13$; $N_{inhibitory} = 14$). Data are expressed as average \pm SEM. Empty squares represent individual values. For more details see Extended Data Tables to Figure 3. KO, knock-out; RIT, resident intruder test; SIT, social interaction test; VGLuT3, vesicular glutamate transporter type 3; WT, wild-type. $\#\#p < 0.01$ versus mouse; $*p < 0.01$ versus WT; $==p < 0.01$ versus control; $@p < 0.05$ versus excitatory; $\bar{p} < 0.01$ versus inhibitory.

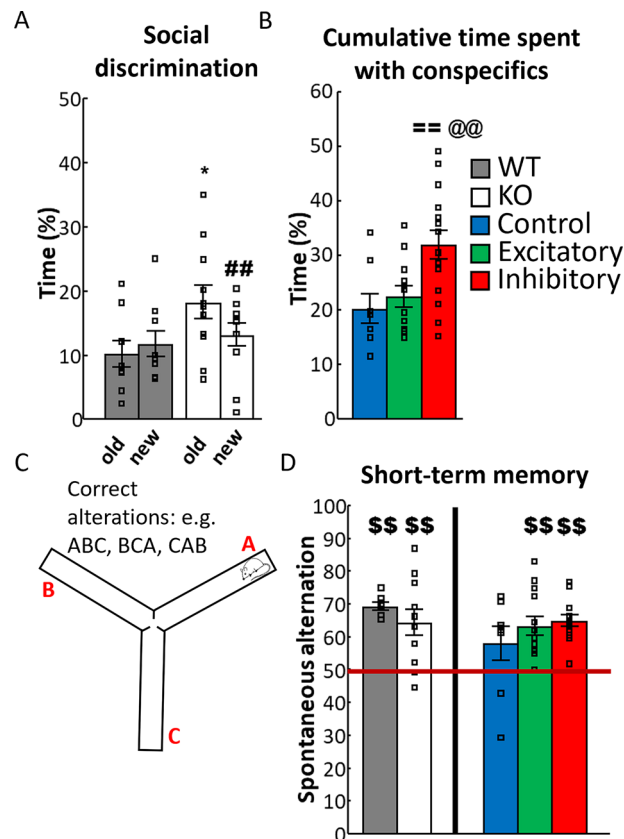


Figure 4. Results of social and working memory experiments. **A**, SDT conducted 1 d after sociability test (Fig. 2A) showed a preference for the familiar, “old” mouse in VGLuT3 KO mice (repeated-measures ANOVA; $N_{WT} = 10$; $N_{KO} = 11$). **B**, In SDT for VGLuT3-Cre mice, there were no differences between the groups regarding their social memory (repeated-measures ANOVA), but the cumulative time spent with social stimuli showed an increased social interest in the inhibitory group (one-way ANOVA; $N_{control} = 8$; $N_{excitatory} = 12$; $N_{inhibitory} = 15$). **C**, Schematic figure of Y-maze test. Three identical arms placed perpendicular can be freely explored by the experimental animal for 5 min. Proper working memory is reflected by consecutive, different arm entries, called spontaneous alternation. **D**, All groups had intact working memory compared with random 50% except for the VGLuT3-Cre control group (single sample *t* test; $N_{WT} = 10$; $N_{KO} = 11$; $N_{control} = 8$; $N_{excitatory} = 13$; $N_{inhibitory} = 14$). Data are expressed as average \pm SEM. Empty squares represent individual values. For more details see Extended Data Tables to Figure 4. KO, knock-out; SDT, social discrimination test; VGLuT3, vesicular glutamate transporter type 3; WT, wild-type. $^{##}p < 0.01$ versus “old” mouse; $^{$$}p < 0.01$ versus random 50; $^{==}p < 0.01$ versus control; $^{@@}p < 0.01$ versus excitatory.

The Ni-DAB-stained slices were evaluated with Olympus DP70 light microscope (4 \times magnification). The virus expression was examined between -4.04 and -4.96 mm from bregma. In case of no or unilateral staining, or infected other brain regions (e.g., dorsal raphe), the test animal and associated data were excluded from the statistical analysis (17/53; Fig. 1B).

To verify whether only VGLuT3+ cells in the MRR expressed the virus, double immunofluorescent staining was conducted (Chaves et al., 2022). For two nights, slides were incubated in anti-RFP (1:1,000, rat, #5f8-100, ChromoTek) and anti-VGLuT3 (1:600, rabbit, #135203, Synaptic Systems) primer solutions on 4 $^{\circ}$ C, then in secondary anti-rabbit antibody conjugated with Alexa-488 (1:500, goat, #111-545-003, Jackson), and anti-rat antibody conjugated with Alexa-594 (1:1,000, goat, #A11029, Invitrogen). Slices were mounted with gelatine and covered with Mowiol (Sigma-Aldrich). The double immunofluorescent staining was evaluated by C2 confocal laser-scanning microscope (Nikon Europe; 20 \times magnification; Fig. 1C).

c-Fos cell counting in brain sites relevant to social behavior and well-known projection areas of MRR (prelimbic cortex, infralimbic cortex and anterior cingulate, medial septum, CA1, CA2, and dentate gyrus) as well as in MRR was also done by Ni-DAB staining. Slices were incubated in the anti-c-Fos primer solution (1:1,000, rabbit, #sc-52, Santa Cruz) for two nights on 4 $^{\circ}$ C. The rest of the protocol was the same as described above. The stained slices were scanned by Panoramic MIDI II Slide scanner (3DHISTECH) and cell bodies (three slides/animal) were counted by ImageJ.

Human brain samples

The study was approved by the Hungarian Medical Research Council – Scientific and Research Ethical Committee (#40197-2/2019/EKU), in accordance with the Ethical Rules for Using Human Tissues for Medical Research in Hungary (HM 34/1999) and the Code of Ethics of the World Medical Association (Declaration of Helsinki). Postmortem brain samples were obtained from the Human Brain Tissue Bank, Semmelweis University. The brains of 11 individuals were used in

the study. Average \pm SEM age was 56.4 ± 54.33 years, while the postmortem delay was 5.72 ± 0.71 -h (for details see Extended Data Table to Fig. 5-3).

Total RNA was isolated by RNeasy Mini Kit (Biomarker) according to the manufacturer's instructions. RNA was diluted into RNase-free water. The quality and quantity of extracted RNA was determined using NanoDrop ND-1000 Spectrophotometer (Thermo Fisher Scientific), and only those with A260/A280 ratio between 1.8 and 2.1 were used in subsequent experiments. The isolated RNA concentration was calculated and normalized with RNase-free water and reverse transcribed into cDNA using SuperScript II reverse transcriptase kit (Invitrogen). After 10-fold dilution, 2.5 μ l of the resulting cDNA was used as template in PCR reactions using SYBR Green dye (Sigma). The PCR reactions were performed on CFX-96 C1000 Touch Real-Time System (Bio-Rad Laboratories) with iTaq DNA polymerase (Bio-Rad Laboratories) in total volumes of 12.5 μ l under the following conditions: 95°C for 3 min, followed by 35 cycles of 95°C for 0.5 min, 60°C for 0.5 min, and 72°C for 1 min. A melting curve was performed at the end of amplification cycles to verify the specificity of the PCR products. All the measurements were conducted in duplicates. The primers used for RT-qPCR were synthesized by Integrated DNA Technologies and used at 300 nM final concentration. Sequences of intron spanning primers were designed based on the common parts of the two splice variants (NM_001145288.2 and NM_139319.3, 122nt-3834nt) to eliminate detection of genomic DNA. The forward primer was GTCTGTCCCCTCATTGTCCGG, while the reversed primer was CACAATTCTGGGAGGTGGCT, with an expected product size of 280 bp. Final cDNA products were sequenced by BIOMI and showed matching to the originally used primers (available upon request). One-third of the amplified PCR product was loaded in agarose gel (1.2%) containing Eco Safe nucleic acid staining solution (1:20,000, Pacific Image Electronics) and the electrophoresis was conducted in 1 \times TAE (40 mM Tris-acetate, 1 mM EDTA, pH 8.0) buffer. The applied separation voltage was 100 V. After the electrophoresis, the DNA bands were visualized by UV transillumination.

Statistical analysis

StatSoft 13.4 software was used. Outliers were defined as data points outside the interval of group mean $\pm 2\times$ standard deviation for the given parameter and thus, were excluded from the analysis. This outlier analysis revealed uncharacteristic behavior resulted in the exclusion of the following number of animals: one WT mouse in the OF test; three WT mice in the Y-maze test; and one WT and one KO mice in sociability and SDTs. Similarly, in the case of VGluT3-Cre mice, the following number of animals were excluded: one mouse in the inhibitory group in the Y-maze test; two mice in the excitatory group during sociability test—object habituation phase, out of which one had to be also excluded from the rest of the experiment (sociability phase, SDT) as well. In the SIT and the EPM test, 1-1 mouse from the excitatory group was excluded. Finally, two mice (one control and one inhibitory) had to be removed from the RIT analysis.

To compare WT and KO animals, we used a *t* test (effect of genotype), while for the behavior of VGluT3-Cre mice, one-way analysis of variance (ANOVA; effect of manipulation) was used. The c-Fos-positive cell counting was done for every brain region separately, as staining was conducted also separately. Therefore, the groups were also compared with *t* test (WT-KO, effect of genotype; VGluT3-Cre control-excitatory, effect of manipulation). However, post hoc correction for multiple comparisons was also done by Benjamini–Hochberg correction (FDR, false discovery rate). SI and spontaneous alteration were tested with single-sample *t* test against 50%, while SD values were tested against 0%. The comparison of sides (left vs right), social preferences in sociability (mouse vs cage), and social discrimination (old vs new) were conducted by mixed-design ANOVA (effect of genotype or manipulation, effect of choice as repeated measure). For aggressive behavior of WT-KO animals in SIT, contingency table was made and Pearson's chi-square test was conducted. Fisher LSD was used for post hoc analysis. Data were expressed as mean \pm SEM and $p < 0.05$ was considered statistically significant, while $0.1 < p < 0.05$ was accepted as a marginal difference.

Results

VGluT3 KO studies

Mobility

There was no difference between the WT and VGluT3 KO animals in the distance moved in OF (Fig. 2B; Extended Data Table to Fig. 2-1), frequency of closed arm entries on EPM (Extended Data Table to Fig. 2-2), or arm entries in Y-maze (Extended Data Table to Fig. 4-2).

Anxiety-like behavior

In the OF, the frequencies of entering different zones did not show any differences. However, the KO animals spent less time in the centrum than the WT ($t_{(18)} = 2.963$; $p = 0.008$; *t* test; Fig. 2C; Extended Data Table to Fig. 2-1). This increased anxiety-like behavior was confirmed on the EPM: KO animals tended to enter the open arm less than the WT (open/total%: $t_{(19)} = 2.019$; $p = 0.058$; *t* test; Fig. 2E; Extended Data Table to Figure 2-2). Additionally, the frequency of rearing (risk assessment) was lower for the KO animals ($t_{(19)} = 2.645$; $p = 0.016$; *t* test). Overall, the KO group exhibited less risk assessment behavior than WT ($RA_{WT} = 67.500 \pm 5.584$; $RA_{KO} = 49.091 \pm 6.511$; $t_{(19)} = 2.125$; $p = 0.047$).

Social interest

During object habituation, KO spent more cumulative time with the two objects than the WT ($F_{(1,17)} = 4.378$; $p = 0.052$) without side preferences. This is also reflected by the reduced time spent with “other” behavior in KO mice ($t_{(17)} = 2.09$; $p = 0.052$; Extended Data Table to Figure 3-1), during which they did not investigate the two empty cages.

During the sociability phase, a significant difference was detected in sniffing frequencies for the effect of choice ($F_{(1,18)} = 16.503$; $p < 0.001$) and a tendency for genotype \times choice interaction ($F_{(1,18)} = 3.327$; $p = 0.085$; Extended Data Table to Fig. 3-2), indicating preference for a social stimulus. For the percentage of time, there was a significant effect of genotype ($F_{(1,18)} = 6.066$; $p = 0.024$), choice ($F_{(1,18)} = 47.541$; $p < 0.001$), and genotype \times choice interaction ($F_{(1,18)} = 5.246$; $p = 0.034$), supporting the frequency data. Post hoc analysis confirmed social preference in both genotypes (WT: $p = 0.006$; KO: $p < 0.001$). Moreover, KO mice spent more time with the conspecific than the WT ($p = 0.002$; Fig. 3A). Additionally, KO group spent less time with “other” behavior ($t_{(18)} = 2.463$; $p = 0.024$), during which they did not investigate the two stimulus cages. Both groups had adequate—over random chance 50%—SI (WT: $t_{(8)} = 3.672$, $p = 0.006$; KO: $t_{(10)} = 10.630$, $p < 0.001$) with significantly higher value in KO animals ($t_{(18)} = -2.087$; $p = 0.051$). These results indicate an increased interest toward conspecifics in the VGLuT3 KO mice.

Social behavior

During SIT frequency of defensive and “other” behavior showed only marginal genotype effect ($t_{(19)} = -1.808$; $p = 0.086$ and $t_{(19)} = -1.936$; $p = 0.068$, respectively; Extended Data Table to Fig. 3-3). However, there was an increase in the percentage of time ($t_{(19)} = -2.182$; $p = 0.042$) and frequency of aggressive behavior ($t_{(19)} = -2.762$; $p = 0.012$) in KO compared with WT. Since the values were low compared with the full length of the test (10 min), our continuous data were transformed into discrete variables: those animals who showed aggression were marked with “yes,” while those who did not were marked with “no” and a contingency table was created. Pearson’s chi-square test showed a significant difference ($\chi^2 = 7.636$; $p = 0.006$): 6 KO animals out of 11 exhibited aggressive behavior, while the WT group showed none (Fig. 3B,C; Extended Data Table to Fig. 3-4).

In RIT, there was no difference between groups, and only a marginal effect of genotype was found in the frequency of defensive behavior ($t_{(19)} = 1.878$; $p = 0.076$; (Fig. 3D,E; Extended Data Table to Fig. 3-5). These results show a context-dependent role of VGLuT3 in aggressive behavior.

Social discrimination

There was a marginal effect of genotype in the percentage of time spent with stimulus animals ($F_{(1,18)} = 3.142$; $p = 0.093$) and a significant genotype \times choice interaction ($F_{(1,18)} = 4.281$; $p = 0.053$). Post hoc analysis of the interaction showed that KO mice spent more time with the already familiar, “old” mouse compared with the WT group ($p = 0.015$) and also compared with the unknown, “new” mouse ($p = 0.031$; Fig. 4A; Extended Data Table to Fig. 4-1). This was also reflected by SD: WT animals did not differ significantly from random chance 0, unlike the KO group ($t_{(10)} = -2.352$; $p = 0.040$). Thus, the SD difference between the groups was significant ($t_{(17)} = 2.503$; $p = 0.023$; Extended Data Table to Fig. 4-1). Nevertheless, their average SD was -19.329 ± 8.217 , which reflects a preference for the “old” mouse.

Working memory

In the Y-maze test, both groups showed higher than random chance spontaneous alteration (WT: $t_{(6)} = 15.154$, $p < 0.001$; KO: $t_{(10)} = 3.608$, $p = 0.005$), indicating intact working memory, without genotype differences (Fig. 4D; Extended Data Table to Fig. 4-2).

Neuronal activity

Ninety minutes after, SIT neuronal activation was measured by c-Fos immunohistochemistry. There was a significant decrease in the number of c-Fos-positive cells in the medial septum ($t_{(11)} = 4.199$; $p = 0.001$) and infralimbic cortex ($t_{(11)} = 3.402$; $p = 0.006$) of VGLuT3 KO mice compared with WT. Other brain areas did not show significant difference after FDR correction (Fig. 5A–D; Extended Data Table to Fig. 5-1).

MRR-VGLuT3 studies

Mobility

MRR-VGLuT3 manipulation only tended to affect the distance traveled in OF ($F_{(2,32)} = 3.04$; $p = 0.062$; Fig. 2B; Extended Data Table to Fig. 2-3). Post hoc analysis showed that the inhibitory group moved less compared with control ($p = 0.082$) and excitatory groups ($p = 0.029$). Moreover, on EPM (Extended Data Table to Fig. 2-4) and in Y-maze (Extended Data Table to Fig. 4-4), the locomotion did not differ between the groups.

Anxiety-like behavior

In the OF, neither the frequencies nor the percentage of time spent in the centrum differed between the groups (Fig. 2C; Extended Data Table to Fig. 2-3). On the other hand, on the EPM MRR-VGLuT3 manipulation significantly influenced the open/total% values ($F_{(2,32)} = 3.828$; $p = 0.032$). According to the post hoc analysis, the excitatory group

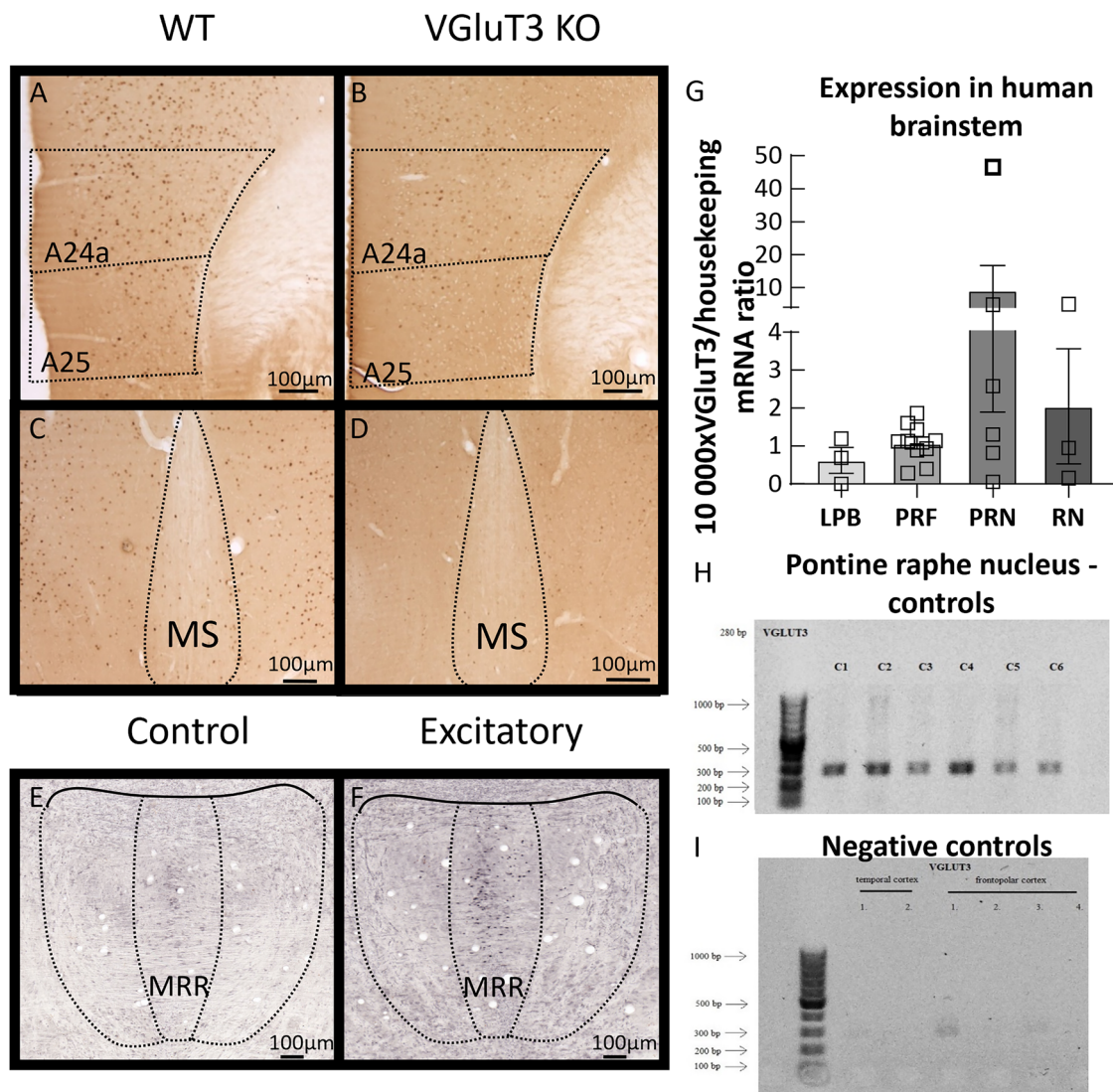


Figure 5. c-Fos staining in the mouse brain and VGLUT3 mRNA expression in healthy human samples. **A–D**, There are decreased numbers of c-Fos-positive cells in the KO (**B,D**) compared with WT (**A,C**) mice in the mPFC (**A,B**) and MS (**C,D**) after SIT ($N_{WT} = 5$; $N_{KO} = 8$). **E,F**, Functional DREADD excitation is reflected by increased c-Fos activity in the MRR of VGLUT3-Cre mice ($N_{control} = 6$; $N_{excitatory} = 3$). Scale bar, 100 μ m. **G**, Relative expression of VGLUT3 mRNA to the measured housekeeping gene (GAPDH) in the investigated brainstem areas (LPB: $N = 3$; PRF: $N = 10$; PRN: $N = 6$; RN: $N = 3$). **H**, After RT-qPCR, samples containing VGLUT3 cDNA were run with gel electrophoresis and sequencing (BIOMI) to validate the specificity of primers. Brain samples from pontine raphe nuclei, which contain the human equivalent of mouse MRR, all expressed VGLUT3 ($N = 6$). **I**, Different cortical areas of healthy human samples were used as negative controls ($N = 6$). Data are expressed as average \pm SEM. Empty squares represent individual values. For more details see Extended Data Tables to Figure 5. bp, base pair; DREADD, designer receptors exclusively activated by designer drugs; KO, knock-out; LPB, lateral parabrachial nucleus; mPFC, medial prefrontal cortex; MRR, median raphe region; MS, medial septum; PRF, pontine reticular formation; PRN, pontine raphe nucleus; RN, midbrain raphe nuclei; RT-qPCR, reverse transcription quantitative polymerase chain reaction; SIT, social interaction test; VGLUT3, vesicular glutamate transporter type 3; WT, wild-type.

entered the open arms more often than control group ($p = 0.009$; Fig. 2E; Extended Data Table to Fig. 2-4). The frequency of rearing showed a tendency ($F_{(2,31)} = 2.769$; $p = 0.078$), while head dipping was significantly influenced by MRR-VGLUT3 manipulation ($F_{(2,31)} = 3.572$; $p = 0.040$). Post hoc test of head dipping revealed an increase in the excitatory group compared with both control and inhibitory groups ($p < 0.05$). Based on this, the excitation of MRR-VGLUT3 neurons was proved to be anxiolytic.

Social interest

During object habituation, there was a marginal effect of choice ($F_{(1,32)} = 3.990$; $p = 0.055$), without significant post hoc effects between the two empty cages (Extended Data Table to Fig. 3-6), and thus, we did not apply correction for side preference during subsequent analysis.

During sociability phase, frequencies only showed significant effect of choice ($F_{(1,32)} = 33.030$; $p < 0.001$), indicating that all animals preferred the stimulus animal, regardless of MRR-VGluT3 manipulation (Extended Data Table to Fig. 3-7). However, percentage of time spent with the stimulus mouse was significantly influenced by MRR-VGluT3 manipulation ($F_{(2,32)} = 6.002$; $p < 0.006$) and choice ($F_{(1,32)} = 88.767$; $p < 0.001$). Post hoc analysis revealed that all mice spent more time with the conspecific ($p < 0.001$). Moreover, the excitatory group spent less time with the two cages together compared with inhibitory group ($p < 0.001$; Fig. 3A). Additionally, there was a significant effect of MRR-VGluT3 manipulation for percentage of time spent with “other” behavior ($F_{(2,32)} = 5.580$; $p = 0.008$), during which the test mice did not investigate the two stimulus cages. More precisely, the excitatory group spent more time with “other” behavior than the inhibitory group ($p = 0.002$). All three groups had adequate, higher than 50% SI (control: $t_{(7)} = 13.670$, $p = 0.001$; excitatory: $t_{(11)} = 7.324$, $p < 0.001$; inhibitory: $t_{(14)} = 6.658$, $p < 0.001$), indicating preference for social stimulus, without differences between the groups (Extended Data Table to Fig. 3-7).

Social behavior

In SIT, there was a marginal effect of MRR-VGluT3 manipulation in the frequency of social behavior ($F_{(2,32)} = 2.702$; $p = 0.082$; Extended Data Table to Fig. 3-8). The frequency of “other,” nonsocial behavior had a significant effect of MRR-VGluT3 manipulation ($F_{(2,32)} = 4.089$; $p = 0.026$), with higher levels in the inhibitory than in control ($p = 0.030$) or excitatory groups ($p = 0.018$). Additionally, MRR-VGluT3 manipulation tended to influence the percentage of time spent with “other,” nonsocial behavior as well ($F_{(2,32)} = 2.613$; $p = 0.089$; Extended Data Table to Fig. 3-8).

During RIT, MRR-VGluT3 manipulation significantly influenced social behavior ($F_{(2,31)} = 5.938$; $p = 0.006$). Post hoc test revealed that the inhibitory group initiated fewer social contacts compared with control ($p = 0.003$) and excitatory ($p = 0.024$) groups. The frequency of “other,” nonsocial behavior was also significantly influenced ($F_{(2,31)} = 5.308$; $p = 0.010$); the inhibitory group had lower frequency compared with control ($p = 0.005$) and excitatory ($p = 0.025$) groups (Fig. 3D,F; Extended Data Table to Fig. 3-9).

Social discrimination

None of the groups could differentiate between the stimulus animals (Extended Data Table to Fig. 4-3). However, there was a significant effect of MRR-VGluT3 manipulation in both the frequencies of interaction ($F_{(2,32)} = 3.336$; $p = 0.048$) and percentage of time spent with it ($F_{(2,32)} = 7.070$; $p = 0.003$). Post hoc test showed that inhibitory group had greater interaction frequencies compared with control ($p = 0.020$), which differed marginally from the excitatory groups ($p = 0.092$; Extended Data Table to Fig. 4-3). In the meantime, post hoc test revealed that the inhibitory group spent more time with the two conspecifics together compared with both control ($p = 0.003$) and excitatory groups ($p = 0.005$; Fig. 4B; Extended Data Table to Fig. 4-3). Accordingly, the frequency ($F_{(2,32)} = 2.586$; $p = 0.091$) and percentage of time ($F_{(2,32)} = 6.526$; $p = 0.004$) spent with “other,” nonsocial behavior showed marginal effect of MRR-VGluT3 manipulation. Post hoc analysis confirmed that the inhibitory group initiated less often (frequency) and spent less time with nonsocial behavior compared with control ($p = 0.004$) and excitatory ($p = 0.007$) groups. Interestingly, this increase in social interest (reflected by the higher time spent with both stimulus animals) was observable 24 h after MRR-VGluT3 inhibition was induced during sociability test.

Working memory

Spontaneous alteration was intact for the MRR-VGluT3 manipulated groups (excitatory: $t_{(12)} = 4.795$, $p < 0.001$; inhibitory: $t_{(12)} = 8.475$, $p < 0.001$; single-sample t test against 50), but not for control group (control: $t_{(7)} = 1.605$, $p = 0.153$; Fig. 4D). However, in direct comparison, there were no significant differences between the groups (Extended Data Table to Fig. 4-4).

Neuronal activity

Only the MRR region showed statistically significant neuronal activation. As expected, after CNO injection, we could detect increased number of c-Fos-positive cells in the stimulatory DREADD group compared with control virus injected one ($t_{(7)} = -14.987$; $p < 0.001$; Fig. 5E,F), confirming that the excitatory DREADD receptors were functional and induced neuronal activation. However, its projection areas did not show increased neuronal activity (Extended Data Table to Fig. 5-2).

Human brain PCR results

VGluT3 mRNA levels were investigated in four human brainstem areas: lateral parabrachial nucleus, pontine reticular formation, pontine raphe nucleus, and midbrain raphe nuclei (Fig. 5G). As negative control, temporal and frontopolar cortex samples were used (Fig. 5H,I). All examined brainstem areas—but not the cortical regions—expressed VGluT3 mRNA (Extended Data Table to Fig. 5-3 and 5-4), indicating possible clinical relevance of our study.

Discussion

We examined the role of VGLuT3+ neurons in social behavior, and—as possible confounding factors—in mobility, anxiety-like behavior and short-term memory in mice. For the short summary of the main findings, see Table 1.

During previous studies, the complete lack of VGLuT3 resulted in deafness (Seal et al., 2008), highly anxious behavior phenotype (Amilhon et al., 2010; Balazsfi et al., 2016; Sakae et al., 2019), altered fear, and stress reactivity (Horvath et al., 2018; Balazsfi et al., 2018a). KO mice proved to be hyperactive, which is circadian dependent and only appears during their active, dark period (Gras et al., 2008; Divito et al., 2015). However, during short observations in a new, aversive (lighted) environment, they might move even less than the controls (Horvath et al., 2018; Balazsfi et al., 2018a; Fazekas et al., 2019; Sakae et al., 2019; de Almeida et al., 2023). Compared with our previous studies (Balazsfi et al., 2018a; Fazekas et al., 2019), in this current project the experiments were done during active period. This could possibly explain why we found no hypoactivity, and the shortness of observation (5 min compared with, for example, 5 h; Gras et al., 2008) could stand behind the undetectability of hyperactivity. Nevertheless, this experimental set-up further confirms the circadian-dependent role of VGLuT3 in locomotion.

It is already well accepted in the literature that the constitutive lack of VGLuT3 throughout the lifetime of mice results in a highly anxious behavioral phenotype (Amilhon et al., 2010; Balazsfi et al., 2016; Sakae et al., 2019). Accordingly, we showed on EPM that VGLuT3 KO mice also exhibited less risk assessment behavior. Moreover, even though OF was conducted in dark, less anxiogenic context, KO animals still preferred the periphery.

In the sociability test, KO animals proved to be more social, which we failed to observe in our previous study (Fazekas et al., 2019). This could be explained by the previously mentioned circadian difference, as well as by slight difference in the protocol. Interestingly, the KO animals showed aggressive behavior only during SIT, which might be explained by the protocol. Although the habituation to the context of SIT is aimed to reduce aggression, the test was conducted in an anxiogenic (lighted) environment, which could have facilitated aggression in the sensitive KO mice, which is known to exhibit high anxiety-like behavior (Amilhon et al., 2010). In accordance with the literature (Amilhon et al., 2010), in RIT there was no significant change in their behavior, further supporting the anxiety-induced nature of aggression during SIT.

Another group linked decreased VGLuT3 protein expression to impaired memory (Cheng et al., 2011). We also found KO mice to be worse in certain aspects of learning, such as working memory and cognitive flexibility (Fazekas et al., 2019). A new study on them confirmed their proper learning and recognition memory ability but impaired pattern separation after aversive stimuli (de Almeida et al., 2023). In the SDT, the VGLuT3 KO animals had impaired long-term (24 h) social memory. Similarly, in our previous study VGLuT3 KO mice showed inadequate long-term (24 h) social memory in the three-chamber sociability test. However, in the Y-maze, which measures working memory, we failed to observe the previously detected impairment (Fazekas et al., 2019). Since the lack of difference was observed during the active phase without hypolocomotion in the present study, but a previous one showed marked hypolocomotion during their inactive phase (de Almeida et al., 2023), this indicates a major sensitivity of these tests to environmental factors, as well as suggest that the KO-induced changes are subtle and can be easily compensated.

Interestingly, social behavior elicited lower neuronal activation in KO than in WT on relevant brain areas (infralimbic cortex and the medial septum). These are projection target of MRR (Leranth and Vertes, 1999; Vertes et al., 1999; McKenna

Table 1. Summary of the main findings

Experiment	Knock-out	MRR excitation	MRR inhibition
Mobility	OF	∅	↓
	EPM	∅	∅
	Y-maze	∅	∅
Anxiety	OF	↑	∅
	EPM	↑	∅
Social behavior	Social interest	↑ (sociability, tendency in SDT)	↓ (indirect during sociability)
	Friendly behavior	∅	↓ in aggressive context (RIT)
	Aggressive behavior	↑ in anxiogenic context (SIT)	∅
Memory	SDT	↓ 24 h SDT	∅
	Y-maze	∅	∅
c-Fos activity	↓ in anterior cingulate, infralimbic cortex and medial septum	↑ in the MRR	-

The results are presented in comparison with their respective control groups: that is, VGLuT3 wild-type littermates for knock-out mice and control group (expressing only RFP in the VGLuT3+ neurons in the MRR) for the excitatory (Gq DREADD + RFP) and inhibitory (Gi DREADD + RFP) chemogenetically manipulated groups. ∅, no difference compared with respective control group; -, not applicable; DREADD, designer receptors exclusively activated by designer drugs; EPM, elevated plus maze; MRR, median raphe region; OF, open field; RFP, red fluorescent protein; RIT, resident intruder test; SDT, social discrimination test; SIT, social interaction test; VGLuT3, vesicular glutamate transporter 3.

and Vertes, 2001; Szonyi et al., 2016) indicating that MRR might be a key hub in VGluT3-influenced social behavior. Therefore, we conducted an MRR-focused analysis using VGluT3-Cre mice.

The activity of MRR has been linked to locomotion in numerous occasions. Stimulation of the MRR resulted in a decreased locomotion and a long-term fear memory formation (Bland et al., 2016; Balazsfi et al., 2017). By using different pharmacons (Shim et al., 2014), the effect of MRR on locomotion was partly dopamine receptor (D2) dependent and partly independent. According to our results, the later pathway potentially includes VGluT3+ neuronal (in)activity. However, stimulation was ineffective and the locomotor effect was not detected in all tests. Interestingly, when all VGluT3-positive neurons of the body were excited with chemogenetics, hypolocomotion was detected in the light phase of mice (Kljakic et al., 2022). Based on these and our results, the role of VGluT3-positive neurons in locomotion is complex and MRR is just one brain area which participates in this role.

Anxiety-like behavior is strongly tied to serotonin, which is also present in the MRR. By using mRNA interference specific to the serotonin transporter in the MRR, anxiety-like behavior was increased on EPM (Verheij et al., 2018). In contrast, in our study excitation of VGluT3+ cell of MRR decreased anxiety. This is in line with the increased anxiety of KO mice and can be explained by the vesicle loading role of VGluT3 (Amilhon et al., 2010). Thus, we might assume that excitation of MRR-VGluT3 neurons increased serotonin loading, thereby reducing anxiety. However, this effect is not robust as the phenomenon was not observable in OF and inhibition was ineffective.

As of its role in social behavior, optogenetic stimulation of the whole MRR decreased aggression in the SIT paradigm, which was accompanied by not only increased levels of serotonin but also glutamate in the mPFC (Balazsfi et al., 2018b). In our present experiment, the decreased time spent with the conspecific and the increased time spent with other behavior during the sociability test in the excitatory group indicate a decreased social interest. However, inhibition increased social interest only 1 d after manipulation, during the SDT. Additionally, inhibition affected friendly social behavior in a context-specific manner: in the anxiogenic SIT tended to increase it, while in RIT decreased it. However, despite our expectations we were unable to find any other major role of MRR-VGluT3+ cells in social behavior.

MRR has been implicated in memory numerous times. It has an effect on both theta oscillation (Viana Di Prisco et al., 2002; Bland et al., 2016) and ripple activity of the hippocampus (Wang et al., 2015), known elementary phenomena of memory formation. Moreover, it is known that MRR sends nonserotonergic projections to the medial septum and hippocampus (Aznar et al., 2004; Fortin-Houde et al., 2023), key brain areas of learning and memory (Tsanov, 2018; Jin et al., 2020; Wu et al., 2021). As previously mentioned, excitation of the MRR elicited a fear memory without actual aversive stimulus, while inhibition of the nucleus prevented the memory formation (Balazsfi et al., 2017). Based on these results, it is expected that MRR-VGluT3+ neurons play a role in some sort of learning and/or memory formation processes. Despite this, in the two memory-related experiments (SDT and Y-maze), we failed to identify any effect. Whether they regulate more complex processes still need to be investigated.

In the MRR, the increase in c-Fos-positive neurons was significant after injection, proving two major points: (1) despite the control animals being injected as well, there is no neuronal activation by CNO and (2) the expressed excitatory DREADD receptors were functional.

Interestingly, the excitation and inhibition of the MRR-VGluT3+ neurons did not yield complementary results. However, we must take into consideration that the used DREADDs activated-inhibited different pathways (G_q vs G_i), which could have caused the different outcomes. Moreover, it has been shown that the MRR-VGluT3+ cells are not homogenous. Unfortunately, with chemogenetics we are unable to differentiate between these cells and it is possible that we have seen the interaction of the activity of these cells.

The expression pattern of VGluT3 in the brain is mostly known from rodent studies. In the brainstem, abundant VGluT3 mRNA and protein levels were found in the dorsal and median raphe nuclei, but only punctate pattern in the pontine nuclei (Schafer et al., 2002; Nakamura et al., 2005; Stornetta et al., 2005). Guo et al. (2005) showed VGluT3-positive cells in the cat parabrachial nucleus. Vigneault et al. (2015) conducted in situ hybridization and immunohistochemistry to detect mRNA and protein levels, respectively, of all three types of VGluTs in the human brain on selected brain regions. However, the only brainstem regions they examined were the collective raphe nuclei, highlighting the dorsal raphe and the pons area. In accordance with the literature, they found abundant VGluT3 mRNA and protein expression in the dorsal raphe; however, in the rest of the pons, it was detected only on protein level. By using RT-qPCR on human brain samples, we confirmed the presence of VGluT3 in human brainstem on the mRNA level. Midbrain raphe nuclei, pontine raphe nuclei, pontine reticular formation, and lateral parabrachial nucleus all showed detectable transcripts, while the control cortical samples did not. This is in accordance with the literature on rodents (Fremau et al., 2002; Gras et al., 2002; Schafer et al., 2002; Herzog et al., 2004; Guo et al., 2005; Stornetta et al., 2005; Hioki et al., 2010).

In summary, our experiments showed that the total ablation of the VGluT3 gene shifted the behavior to be socially more active. However, the fact that the KO animal showed increased aggression only during the anxiogenic SIT test, but not during the RIT, suggests that the aggression of these animals was induced by anxiety. We further confirmed the highly anxious phenotype and an impairment in long-term social memory in the VGluT3 KO animals. In the case of VGluT3+ MRR neurons, we found that they play a role in locomotion and long-term social interest. Although in our case it was not possible to differentiate between the VGluT3+ only and VGluT3+/5-HT+ neurons of the MRR, it was demonstrated that either one or both subpopulations can contribute to the anxiolytic effect of MRR but has subtle effect on social behavior.

Data Availability

The datasets generated and/or analyzed during the current study are available from the corresponding author on reasonable request.

References

- Amilhon B, et al. (2010) VGLUT3 (vesicular glutamate transporter type 3) contribution to the regulation of serotonergic transmission and anxiety. *J Neurosci* 30:2198–2210.
- Aznar S, Qian ZX, Knudsen GM (2004) Non-serotonergic dorsal and median raphe projection onto parvalbumin- and calbindin-containing neurons in hippocampus and septum. *Neuroscience* 124:573–581.
- Balazsfi D, Farkas L, Csikota P, Fodor A, Zsebok S, Haller J, Zelena D (2016) Sex-dependent role of vesicular glutamate transporter 3 in stress-regulation and related anxiety phenotype during the early postnatal period. *Stress* 19:434–438.
- Balazsfi DG, et al. (2017) Median raphe region stimulation alone generates remote, but not recent fear memory traces. *PLoS One* 12: e0181264.
- Balazsfi D, Fodor A, Torok B, Ferenczi S, Kovacs KJ, Haller J, Zelena D (2018a) Enhanced innate fear and altered stress axis regulation in VGLUT3 knockout mice. *Stress* 21:151–161.
- Balazsfi D, et al. (2018b) Differential roles of the two raphe nuclei in amiable social behavior and aggression - an optogenetic study. *Front Behav Neurosci* 12:163.
- Biro L, Toth M, Sipos E, Bruzsik B, Tulogdi A, Bendahan S, Sandi C, Haller J (2017) Structural and functional alterations in the prefrontal cortex after post-weaning social isolation: relationship with species-typical and deviant aggression. *Brain Struct Funct* 222:1861–1875.
- Bland BH, Bland CE, MacIver MB (2016) Median raphe stimulation-induced motor inhibition concurrent with suppression of type 1 and type 2 hippocampal theta. *Hippocampus* 26:289–300.
- Calizo LH, Akanwa A, Ma X, Pan YZ, Lemos JC, Craige C, Heemstra LA, Beck SG (2011) Raphe serotonin neurons are not homogenous: electrophysiological, morphological and neurochemical evidence. *Neuropharmacology* 61:524–543.
- Chaves T, Torok B, Fazekas CL, Correia P, Sipos E, Varkonyi D, Hellinger A, Erk D, Zelena D (2022) Median raphe region GABAergic neurons contribute to social interest in mouse. *Life Sci* 289:120223.
- Cheng XR, Yang Y, Zhou WX, Zhang YX (2011) Expression of VGLUTs contributes to degeneration and acquisition of learning and memory. *Neurobiol Learn Mem* 95:361–375.
- Dahlstrom A, Fuxe K (1964) Localization of monoamines in the lower brain stem. *Experientia* 20:398–399.
- de Almeida C, Chabbah N, Eyraud C, Fasano C, Bernard V, Pietrancosta N, Fabre V, El Mestikawy S, Daumas S (2023) Absence of VGLUT3 expression leads to impaired fear memory in mice. *eNeuro* 10.
- Divito CB, et al. (2015) Loss of VGLUT3 produces circadian-dependent hyperdopaminergia and ameliorates motor dysfunction and l-Dopa-mediated dyskinesias in a model of Parkinson's disease. *J Neurosci* 35:14983–14999.
- Fazekas CL, et al. (2019) Consequences of VGLUT3 deficiency on learning and memory in mice. *Physiol Behav* 212:112688.
- Fazekas CL, Bellardie M, Torok B, Sipos E, Toth B, Baranyi M, Sperlagh B, Dobos-Kovacs M, Chaillou E, Zelena D (2021) Pharmacogenetic excitation of the median raphe region affects social and depressive-like behavior and core body temperature in male mice. *Life Sci* 286:120037.
- Fortin-Houde J, Henderson F, Dumas S, Ducharme G, Amilhon B (2023) Parallel streams of raphe VGLUT3-positive inputs target the dorsal and ventral hippocampus in each hemisphere. *J Comp Neurol* 531:702–719.
- Fremeau RT Jr, et al. (2002) The identification of vesicular glutamate transporter 3 suggests novel modes of signaling by glutamate. *Proc Natl Acad Sci U S A* 99:14488–14493.
- Gras C, Herzog E, Bellenchi GC, Bernard V, Ravassard P, Pohl M, Gasnier B, Giros B, El Mestikawy S (2002) A third vesicular glutamate transporter expressed by cholinergic and serotonergic neurons. *J Neurosci* 22:5442–5451.
- Gras C, et al. (2008) The vesicular glutamate transporter VGLUT3 synergizes striatal acetylcholine tone. *Nat Neurosci* 11:292–300.
- Guo ZL, Moazzami AR, Longhurst JC (2005) Stimulation of cardiac sympathetic afferents activates glutamatergic neurons in the parabrachial nucleus: relation to neurons containing nNOS. *Brain Res* 1053:97–107.
- Herzog E, Gilchrist J, Gras C, Muzerelle A, Ravassard P, Giros B, Gaspar P, El Mestikawy S (2004) Localization of VGLUT3, the vesicular glutamate transporter type 3, in the rat brain. *Neuroscience* 123:983–1002.
- Hioki H, Nakamura H, Ma YF, Konno M, Hayakawa T, Nakamura KC, Fujiyama F, Kaneko T (2010) Vesicular glutamate transporter 3-expressing nonserotonergic projection neurons constitute a subregion in the rat midbrain raphe nuclei. *J Comp Neurol* 518:668–686.
- Horvath HR, Fazekas CL, Balazsfi D, Jain SK, Haller J, Zelena D (2018) Contribution of vesicular glutamate transporters to stress response and related psychopathologies: studies in VGLUT3 knockout mice. *Cell Mol Neurobiol* 38:37–52.
- Hughes RN (2004) The value of spontaneous alternation behavior (SAB) as a test of retention in pharmacological investigations of memory. *Neurosci Biobehav Rev* 28:497–505.
- Jackson J, Bland BH, Antle MC (2009) Nonserotonergic projection neurons in the midbrain raphe nuclei contain the vesicular glutamate transporter VGLUT3. *Synapse* 63:31–41.
- Jahanshahi A, Steinbusch HW, Temel Y (2013) Distribution of dopaminergic cell bodies in the median raphe nucleus of the rat brain. *J Chem Neuroanat* 53:60–63.
- Jin T, Chen R, Shao M, Yang X, Ma L, Wang F (2020) Dorsal hippocampus- and ACC-projecting medial septum neurons differentially contribute to the recollection of episodic-like memory. *FASEB J* 34:11741–11753.
- Kljakic O, Hogan-Cann AE, Yang H, Dover B, Al-Onaizi M, Prado MAM, Prado VF (2022) Chemogenetic activation of VGLUT3-expressing neurons decreases movement. *Eur J Pharmacol* 935:175298.
- Leranth C, Vertes RP (1999) Median raphe serotonergic innervation of medial septum/diagonal band of Broca (MSDB) parvalbumin-containing neurons: possible involvement of the MSDB in the desynchronization of the hippocampal EEG. *J Comp Neurol* 410:586–598.
- McKenna JT, Vertes RP (2001) Collateral projections from the median raphe nucleus to the medial septum and hippocampus. *Brain Res Bull* 54:619–630.
- Nakamura K, Matsumura K, Kobayashi S, Kaneko T (2005) Sympathetic premotor neurons mediating thermoregulatory functions. *Neurosci Res* 51:1–8.
- Sakae DY, Ramet L, Henrion A, Poirel O, Jamain S, El Mestikawy S, Daumas S (2019) Differential expression of VGLUT3 in laboratory mouse strains: impact on drug-induced hyperlocomotion and anxiety-related behaviors. *Genes Brain Behav* 18:e12528.
- Schafer MK, Varoqui H, Defamie N, Weihe E, Erickson JD (2002) Molecular cloning and functional identification of mouse vesicular glutamate transporter 3 and its expression in subsets of novel excitatory neurons. *J Biol Chem* 277:50734–50748.

- Seal RP, et al. (2008) Sensorineural deafness and seizures in mice lacking vesicular glutamate transporter 3. *Neuron* 57:263–275.
- Shim I, Stratford TR, Wirtshafter D (2014) Dopamine is differentially involved in the locomotor hyperactivity produced by manipulations of opioid, GABA and glutamate receptors in the median raphe nucleus. *Behav Brain Res* 261:65–70.
- Sos KE, Mayer MI, Cserep C, Takacs FS, Szonyi A, Freund TF, Nyiri G (2017) Cellular architecture and transmitter phenotypes of neurons of the mouse median raphe region. *Brain Struct Funct* 222:287–299.
- Stornetta RL, Rosin DL, Simmons JR, McQuiston TJ, Vujovic N, Weston MC, Guyenet PG (2005) Coexpression of vesicular glutamate transporter-3 and gamma-aminobutyric acidergic markers in rat rostral medullary raphe and intermediolateral cell column. *J Comp Neurol* 492:477–494.
- Szonyi A, Mayer MI, Cserep C, Takacs VT, Watanabe M, Freund TF, Nyiri G (2016) The ascending median raphe projections are mainly glutamatergic in the mouse forebrain. *Brain Struct Funct* 221:735–751.
- Szonyi A, et al. (2019) Median raphe controls acquisition of negative experience in the mouse. *Science* 366:46.
- Tsanov M (2018) Differential and complementary roles of medial and lateral septum in the orchestration of limbic oscillations and signal integration. *Eur J Neurosci* 48:2783–2794.
- Turcotte-Cardin V, et al. (2019) Loss of adult 5-HT_{1A} autoreceptors results in a paradoxical anxiogenic response to antidepressant treatment. *J Neurosci* 39:1334–1346.
- Verheij MMM, et al. (2018) Median and dorsal raphe serotonergic neurons control moderate versus compulsive cocaine intake. *Biol Psychiatry* 83:1024–1035.
- Vertes RP, Fortin WJ, Crane AM (1999) Projections of the median raphe nucleus in the rat. *J Comp Neurol* 407:555–582.
- Viana Di Prisco G, Albo Z, Vertes RP, Kocsis B (2002) Discharge properties of neurons of the median raphe nucleus during hippocampal theta rhythm in the rat. *Exp Brain Res* 145:383–394.
- Vigneault E, Poirel O, Riad M, Prud'homme J, Dumas S, Turecki G, Fasano C, Mechawar N, El Mestikawy S (2015) Distribution of vesicular glutamate transporters in the human brain. *Front Neuroanat* 9:23.
- Wang DV, Yau HJ, Broker CJ, Tsou JH, Bonci A, Ikemoto S (2015) Mesopontine median raphe regulates hippocampal ripple oscillation and memory consolidation. *Nat Neurosci* 18:728–735.
- Wu D, et al. (2021) Medial septum tau accumulation induces spatial memory deficit via disrupting medial septum-hippocampus cholinergic pathway. *Clin Transl Med* 11:e428.